



# Organic nanocomposite Band-Aid for chronic wound healing: a novel honey-based nanofibrous scaffold

S. Kanimozhi<sup>1</sup> · Geetha Kathiresan<sup>1</sup> · A. Kathalingam<sup>2</sup> · Hyun-Seok Kim<sup>3</sup> · M. Naveen Rooba Doss<sup>1</sup>

Received: 28 October 2019 / Accepted: 27 December 2019 / Published online: 8 January 2020  
© King Abdulaziz City for Science and Technology 2020

## Abstract

Honey is a natural medicine; incorporating it, a PVA/honey hybrid nanofibrous Band-Aid was fabricated by electrospinning technique, and the prepared electrospun scaffolds were characterized by UV–visible spectroscopy, FTIR spectroscopy and XRD techniques. The honey-adsorbed scaffolds showed UV–visible absorption at 306 nm wavelength expressing the presence of honey in polymer scaffold. In addition, it indicated that the honey was not degenerated even at the highest applied voltage of 16 kV given during electrospinning. Conductivity study of the scaffold revealed linear increase of conductivity as 0.74, 0.80, 0.82 and 0.83 mho with increase of honey concentration, which revealed the high honey releasing profile of the scaffolds at higher concentration. Efficiency of fabricated Band-Aids was analyzed by swelling character and in vitro releasing kinetics. The higher level of honey osmolality increased the fluid uptake into scaffolds and showed highest degree of swelling indicating an efficient release of honey by diffusion.

**Keywords** Honey · Wound healing · Tissue regeneration · Nanocomposite scaffold · Electrospinning · Polyvinyl alcohol Band-Aid

## Introduction

Human skin is very much prone to injuries causing wounds due to environmental factors even on day-to-day activities. Wound healing is an unresolved problem which affects many people by the way of treatment cost and other related socio-economic issues (Long et al. 2018; Nethi et al. 2019; Samarghandian et al. 2017). The wound becomes a major issue for a human due to the lack of disintegration of tissues, and it is classified as acute and chronic wounds based on the degree of damage and duration of healing (Qi et al. 2018; Song and Salcido 2011). Acute wound healing is progressed through the combination of various wound healing mechanisms such

as hemostasis, inflammation, tissue re-epithelization and remodeling (Biswas et al. 2018; Stejskalová and Almquist 2017). However, the prolongation of different stages of normal wound healing results in chronic wounds. The chronic wounds are characterized by the increased levels of ROS, protease, debridement of cells and inflammatory cytokines such as TNF- $\alpha$ , IL-6 with insufficiency of growth factors and ECM degradation accumulated with bacterial infection (Anand et al. 2019). Compared with acute wounds, chronic wounds influence the life of people by causing depression, anxiety, financial burden, pain, inflammation, increased hospital stay, morbidity or even mortality.

In the process of wound healing, wound dressings are playing an indispensable major role in chronic wound management (Hassiba et al. 2017; Sarhan et al. 2016; Yao et al. 2019). The ideal characteristics of wound dressings are adequate water transmission rate, optimal oxygen permeability, provision of moist environment to the wound site, non-toxicity, selective adhesion to normal tissues, appropriate temperature and pH, pain mitigation, reduction of skin irritation, absorption of excess ooze at the wound site and inhibition of bacterial infection, and contaminants (Putu et al. 2018; Son et al. 2019). Bacterial infection at wound region can dampen healing process of wound and leads

✉ Geetha Kathiresan  
rktgeetha@gmail.com

<sup>1</sup> Nanotechnology Division / Department of ECE, Periyar Maniammai Institute of Science and Technology, Thanjavur 613 403, Tamil Nadu, India

<sup>2</sup> Millimeter-Wave Innovation Technology (MINT) Research Center, Dongguk University-Seoul, Seoul 04620, Republic of Korea

<sup>3</sup> Division of Electronics and Electrical Engineering, Dongguk University-Seoul, Seoul 04620, Republic of Korea

to mortality of patient. Anti-bacterial agent-incorporated wound dressing is one of the best ways for treating the bacterial infections without leading to mortality (Neres Santos et al. 2019; Zanier and Bordoni 2015). Inflammatory microenvironment in chronic wounds also delays the healing mechanism which are endowed by the pro-inflammatory cytokines (TNF- $\alpha$ , IL-6), oxidative stress, cyclooxygenase-2 (COX-2), enormous amount of MMPs and lack of growth factors (Movassaghi et al. 2019). Recently, high-efficiency wound healing method was reported based on electrical stimulation by applying small electrical pulses by wearable nano-generator device (Long et al. 2018). The conventional wound healing methods using cotton, linen and synthetic bands are not successfully treating the bacterial infection and ischemia (Lin et al. 2001; Moura et al. 2013). Recently, more attention is given to biomaterials to enhance wound healing mechanisms. Numerous studies are being conducted on wound healing efficiency of natural substances such as thymol, *Garcinia cowa*, *Garcinia mangostana*, alkannin, emu oil, *Stryphnodendron adstringens* (Costa et al. 2019; Pinto et al. 2015; Suwantong et al. 2012).

Honey has been considered for many decades as a natural remedy for wound healing. It has good medicinal values with anti-microbial and fungal activities, which can be used for healing various wounds without any harmful side effects (Albaridi 2019; Kwakman et al. 2010; Maleki et al. 2013). Moreover, it has a variety of nutrients as the bees collect it from various plants and environments. It also contains minerals, vitamins, carbohydrates, proteins, amino acids and lipids that help fast and easy wound healing. Honey accelerates fast healing of wounds by virtue of its nature and contents; it stimulates growth of new tissues by stimulating anti-inflammatory activities. It is a better anti-microbial agent compared to other topical agents; it promotes re-epithelialization without formation of scar. These attractive properties of honey have highly motivated and encouraged to invent a cost-effective and efficient Band-Aid to treat complicated wounds. Additionally, it has anti-inflammatory, anti-oxidant, anti-cancer, anti-diabetic, and immunomodulatory activities which are not available in other substances. The presence of high sugar content, hydrogen peroxide (H<sub>2</sub>O<sub>2</sub>), low pH, high osmotic pressure, low water activity, low protein content, high viscosity and phenolic compounds such as pinocembrin, syringic acid and glucose oxidase has been the main cause for the anti-bacterial activity of honey (Mama et al. 2019; Meo et al. 2017). Honey also contains lysozyme, a well-known powerful anti-microbial agent and defensin-1, anti-microbial peptide showing inhibition against both Gram-positive and Gram-negative bacteria. The existence of peroxidase, catalase, carotenoids and ascorbic acid in honey retains the anti-oxidant properties that neutralize the free radicals and reduce ROS level in chronic wounds (Moore et al. 2001). However, honey-based conventional dressings

(gauze, hydrogel and polyurethane films) are not efficient in producing moist environment, protection against infection, painless removing, and they produce foul smell and bleeding of exudates from the wounds (Lin et al. 2001; Oktay et al. 2014). However, nano-scaffold-based dressings overcome such problems faced by conventional dressings because of excellent soft tissue-mimicking property, high surface area, high porosity, high absorption, high oxygen permeability, anti-fouling property, providing moist environment, scar-free wound healing, reducing pain while removing and safe wound sterilization (Chao et al. 2018; Minden-Birkenmaier and Bowlin 2018). In this direction, synthetic polymer polyvinyl alcohol (PVA) is a very good option considering its biodegradability, physical and chemical properties, and excellent chemical resistance (El-Zaher and Osiris 2005).

Several techniques are available for the synthesis of PVA-based nano-scaffolds including electrospinning, phase separation, template synthesis, freeze-drying, self-assembly and electro-spraying (Anderson et al. 2019; Li et al. 2017). Compared with other techniques, the electrospinning is the most efficient technique for the production of scaffolds with adequate pore size for cellular migration, suitable surface area for cell adhesion, growth, differentiation and proliferation for tissue regeneration application (Hassiba et al. 2017; Rezvani et al. 2016; Wang et al. 2018; Xiao et al. 2018). In the present study, honey--incorporated nanocomposite organic Band-Aids were fabricated by electrospinning technique. This fabricated Band-Aid can provide anti-bacterial, anti-inflammatory, and anti-oxidant properties, and the patients can easily use the Band-Aids in an eco-friendly way with increased bio-compatibility and without any side effects.

## Materials and methods

### Fabrication of PVA nano-scaffolds by electrospinning

Polyvinyl alcohol (PVA) of 13,000–23,000 MW purchased from Sigma-Aldrich and pure honey collected from neem tree located in the campus of PMIST (Periyar Maniammai Institute of Science and Technology) were used in this work. Pure PVA nano-fibrous scaffolds were fabricated as experimented samples to compare morphology and other properties with honey-loaded scaffolds. For the preparation of PVA scaffold, 2 g of PVA was mixed in 25 ml of distilled water in a beaker to obtain 8 wt% and stirred using a magnetic stirrer at 80 °C for 4 h. The resultant solution was loaded into a 10-ml syringe with 22-gauge needle for flow controller. Optimized parameters used for the electrospinning of PVA scaffolds were 0.001 ml/min flow rate, 15 cm distance between collector and syringe, and 15 kV applied voltage.

## Fabrication of PVA/honey organic nano-scaffolds by electrospinning

For the preparation of honey-incorporated PVA solution, 50% diluted honey of different concentrations was added to 8 wt% PVA solution and stirred for 2 h continuously. Four sets of solutions with 1, 2, 3 and 4 ml honey in constant volume of PVA solution (8 wt%) were prepared. The range of different parameters employed to prepare different sets of honey-loaded scaffolds is shown in Table 1. Solution flow rate of 0.06–0.001 ml/min, the distance between collector and syringe 5–20 cm, applied voltage of 10–16 kV and honey concentration 1–4 ml were used keeping constant PVA concentration (8 wt%) and needle size (22 G).

### Optimization of process parameters

For the identification of suitable electrospinning condition, the different parameters such as solution flow rate, distance between collector and syringe, applied voltage and solution concentrations were varied as summarized in Table 1 and their effects are analyzed. Flow rate was varied as 0.06, 0.01, 0.005 and 0.001 ml/min and the low rate of 0.001 ml/min was found suitable to prepare PVA scaffolds with good results. The distance between collector and needle tip is also important in regulating the solvent evaporation rate (SER) for uniform and smooth nanofibrous material preparation, and it was varied as 5, 10, 15 and 20 cm. The electrical voltages applied to electrospinning system were 10, 12, 14, and 16 V; among them, the high voltage of 14 V or 16 V was found suitable for the formation of nanofibrous scaffolds. Similarly, honey concentration was also varied as 1, 2, 3, and 4 ml and found that higher concentration (4 ml) was suitable for the formation of honey-incorporated PVA nano-fiber.

### Characterization of the honey/PVA hybrid nano-fibrous scaffolds

Surface morphology of the synthesized electrospun PVA and PVA/honey nanofibers was characterized using scanning electron microscope (TESCAN, VEGA3 LMU) with different magnifications. Prior to SEM measurement, the samples

**Table 1** Range of various parameters used for the preparation of honey/PVA nano-fibrous scaffolds by electrospinning

Parameters	Range
Flow rate (ml/min)	0.06, 0.01, 0.005 and 0.001
Distance between collector and syringe (cm)	5, 10, 15 and 20
Applied voltage (KV)	10, 12, 14 and 16
Concentration of honey (ml)	1, 2, 3 and 4

were sputtered with gold–palladium. Absorption spectra of all the sample solutions were analyzed by UV–Vis spectroscopy (Mapada, UV1800) in the range of 200–800 nm to identify the composition. Physicochemical properties of the prepared samples were analyzed using Fourier transform infrared spectroscopy (FTIR) with Perkin Elmer (version 10.03.09) FTIR spectrophotometer in the wavenumber range 4000–600/cm. Crystalline nature of the prepared nanofibers was characterized using PAN analytical X' Pert Pro X-ray diffractometer.

### Analysis of nano-fibrous scaffold swelling property

Water absorption ability of PVA/honey nanofiber was studied by measuring the swelling behavior. Two different thickness samples cut into 1 cm × 1 cm area were weighed initially ( $W_i$ ) before starting the experiment at time  $t = 0$ . Then they were kept immersed in 5 ml of PBS saline solution. At desired time intervals (24 h, 48 h and 72 h), the samples were taken out and weighed ( $W_t$ ) again to obtain the swelling ratio. The swelling ratio ( $s$ ) was calculated using the following equation:

$$s = \frac{W_t - W_i}{W_i}, \quad (1)$$

where  $W_i$  is initial weight of the sample before each cycle of swelling analysis and  $W_t$  is the final weight of the swollen sample after analysis.

### In vitro releasing kinetics analysis

For in vitro releasing kinetics of honey from scaffolds, two scaffolds fabricated from two different deposition time 2 h and 4 h with different thicknesses weighed initially were immersed in two separate 10 ml deionized water and kept undisturbed for 24 h in a shaker at 37°C. At the end of 24 h, a solution of 3–5 ml from the two different mediums was removed and the kinetics study was done using UV–visible spectrophotometer (Mapada, UV1800) in the wavelength range of 200–800 nm. The solution was returned to their respective mediums. At the desired duration, the solution of 3–5 ml was removed and the analysis was repeated again. The quantity of honey release was determined by its concentration in the medium and their relation with two different thickened samples was compared.

### MTT cytotoxicity assay

Cytotoxicity of PVA and PVA/honey nanofibers of different honey concentration was evaluated using L929 skin fibroblast cell lines of male mouse. Nanofibers of PVA with four various concentrations of honey were peeled from the aluminum foil and 1 mg was collected; both sides of the fibers

were sterilized using UV light in a laminar airflow chamber for 1 h. The honey from the fibers was extracted by soaking the fibers in the culture medium of DMEM with 10% fetal bovine serum and 1% antibiotic (penicillin–streptomycin) at room temperature for 24 h. 1 mg/ml of fiber's solution was prepared for the cytotoxic analysis.

The cytotoxic analysis was done by adding 100  $\mu$ l of fiber solution to 96-well plates cultured with cells. L929 fibroblast cell line at 10,000–20,000 cells/well was seeded into 96-well plates before adding fiber solution and then it was incubated in a CO<sub>2</sub> incubator with 5% CO<sub>2</sub> for 48 h. After 48 h, the fiber solution of each concentration was added to the cells seeded in each well followed by twofold dilution ranging from higher concentration to lower concentration. The flowchart of PVA/honey nanofibrous scaffold fabrication is presented in Fig. 1.

Cell viability and cytotoxicity of the samples were evaluated using MTT [3-(4,5-dimethylthiazole-2-yl)-2,5-diphenyltetrazolium bromide] assay. Mitochondria reductase enzyme in the viable cells reduces the tetrazolium salts to formazan crystals. The amount of live cells in each well is proportional to the amount of formazan crystals formed in the well. The medium from the well was removed and 100  $\mu$ l of MTT solution (5 mg/ml of MTT in DMEM) was added. MTT-added plates were incubated for 3–4 h in an incubator at 37 °C. Then again the medium (MTT + medium) was removed and the same quantity of DMSO was added to dissolve the formed formazan crystals in the well. After 20 min, the absorbance was measured using ELISA plate counter to evaluate the quantity of viable cells. The absorbance is directly proportional to the amount of formazan crystal formed in each wells. The cell viability can be calculated using the following equation:

$$\text{Cell viability} = (\text{Absorbance in treatment}/\text{Absorbance in control}) \times 100. \quad (2)$$

## Results and discussion

### Effect of flow rate on PVA/honey nanofiber morphology

Solution flow rate is an important parameter affecting formation of nanofiber in the electrospinning process. The variation in solution flow rate modifies size and shape of droplets formed at the tip of needle inducing changes in morphology of fiber formed. To optimize the flow rate, it was initially tried with 0.06, 0.01, 0.005 and 0.001 ml/min flow rates and recognized that a very low flow rate was suitable to form smooth and uniform nanofibers. Figure 2a–d shows the SEM images of PVA/honey nanofiber formed at 0.06, 0.01, 0.005, and 0.001 ml/min, respectively. For the flow rate of 0.06 ml/min, large volume of solution was ejected from the spinneret and deposited over the collector as thick particles without fibrous nature. As shown in Fig. 2a, the higher flow rate of 0.06 ml/min led to the solution drop down as a normal fluid without forming any fiber, which is indicated in SEM morphology as spherical-shaped particles. The decrease in flow rate of 0.01 ml/min produced a chain-like structure of the particles deposited, whereas the slow rates 0.005 and 0.001 ml/min produced stable Taylor cone forming smooth and uniform collection of fibrous material on the collector plate (Fig. 2c, d). The very slow rate 0.001 ml/min revealed the formation of thin and smooth fiber as shown in Fig. 2d. Zargham et al. also experienced 0.001 ml/min as the optimum flow rate for smooth formation of fibers (Zargham et al. 2012). At the same time, too low flow rate is also not good to maintain the shape of Taylor cone and

**Fig. 1** Fabrication flowchart of PVA/honey organic nanoscaffold

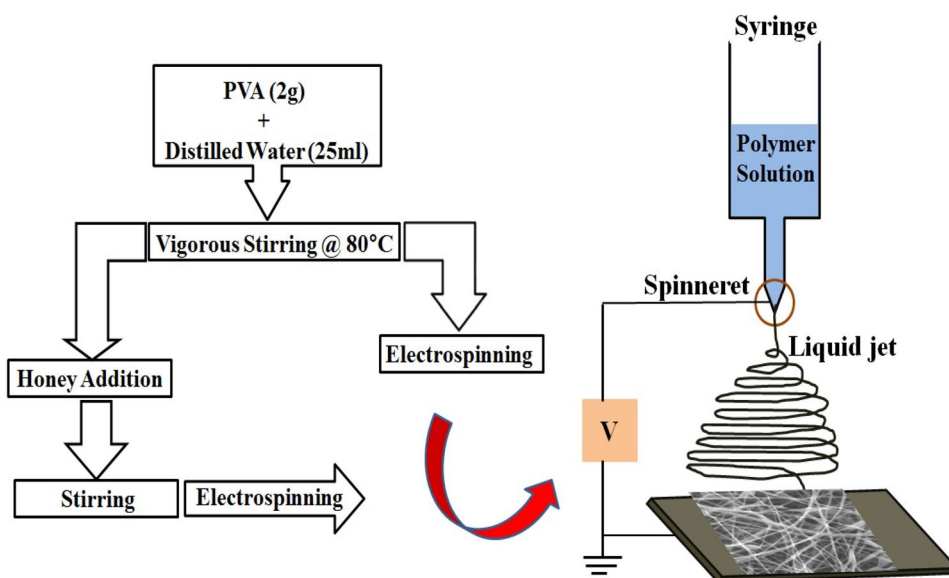
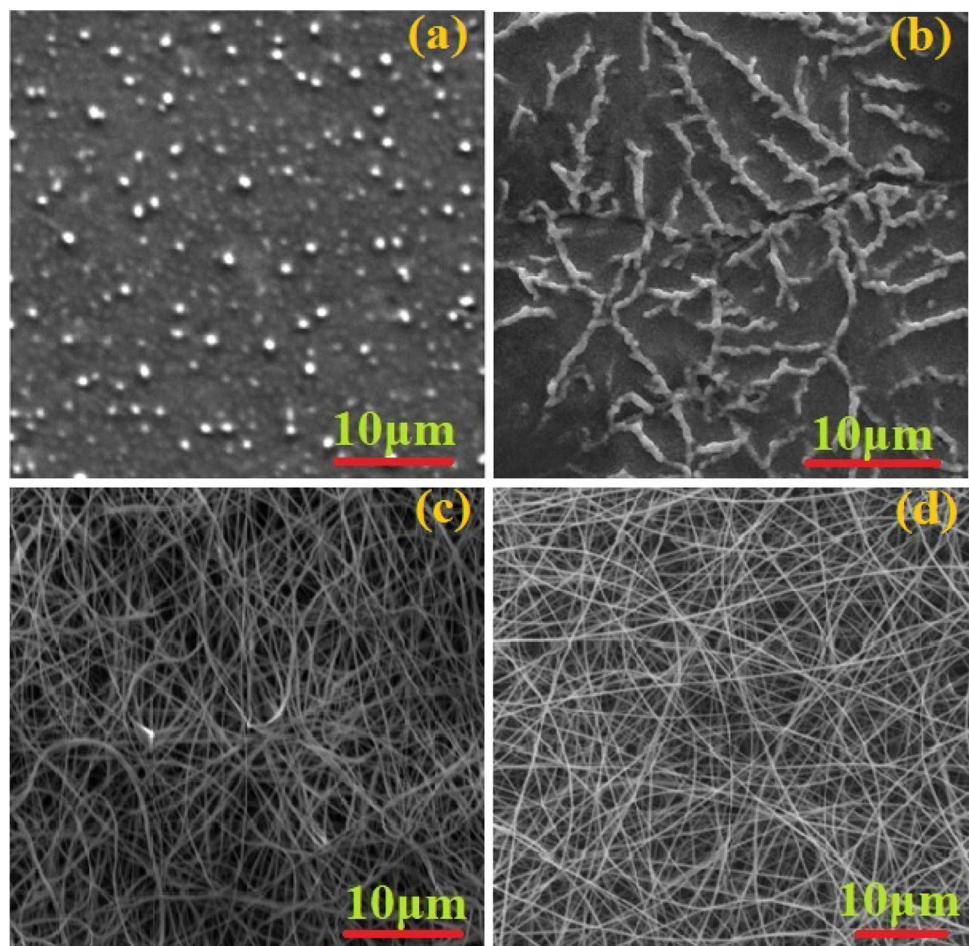


**Fig. 2** SEM image of nanofibers formed at **a** 0.06 ml/min, **b** 0.01 ml/min, **c** 0.005 ml/min and **d** 0.001 ml/min flow rates



not sufficient solution was ejected for Taylor cone formation (Gupta et al. 2016). Morphology of cross-linked fibers uniformly distributed with less defect was shown at this slow flow rate justifying the optimum flow rate for formation of fiber. Hence, in this electrospinning process a minimum flow rate of 0.001 ml/min was used for further process of fibers.

### Effect of collector and tip distance on nanofiber formation

The distance between collector and syringe tip has direct effect on the evaporation of solvent and jet ejection for the formation of uniform and well-formed fibers. Hence, an ideal distance between collector and tip of the needle is very important to regulate the solvent evaporation rate (SER). The SER plays a major role in fiber diameter and fiber morphology of nanofibrous scaffold formation. The distance was changed to 5, 10, 15 and 20 cm and their role in the formation of nanofibrous scaffold was observed. As shown in Fig. 3a, b, thick fibers with bead structure are formed for shortest distance 5 cm as observed. This is

because, at a short distance (5 cm), solution was dropped onto the collector without forming fiber as there was no sufficient distance for solvent evaporation due to shorter distance, whereas a longer distance of 10 cm resulted in fiber structure without drop down of solvent, but web-like defective structures (Fig. 3c). However, compared to 5 and 10 cm distances, 15 and 20 cm distances produced better result in the formation of fiber without any residual solvent and defective morphological structures. Among 15 and 20 cm distances, the 15 cm produced a smoother and continuously organized cross-linked fiber structures (Fig. 3d). This longer distance permits complete evaporation of solvent before reaching the collector resulting good fibrous scaffolds. However, the very large distance of 20 cm resulted in uneven thick fiber structure with large breakage and dense coverage (Fig. 3e) compared to 15 cm. This morphological analysis suggests that increase of distance between collector and tip to an optimum value would provide suitable time for solvent evaporation and proper ejection of fluid jet whereas increase or decrease of distance from optimum value would produce defects in morphology of electrospun nanofibers.

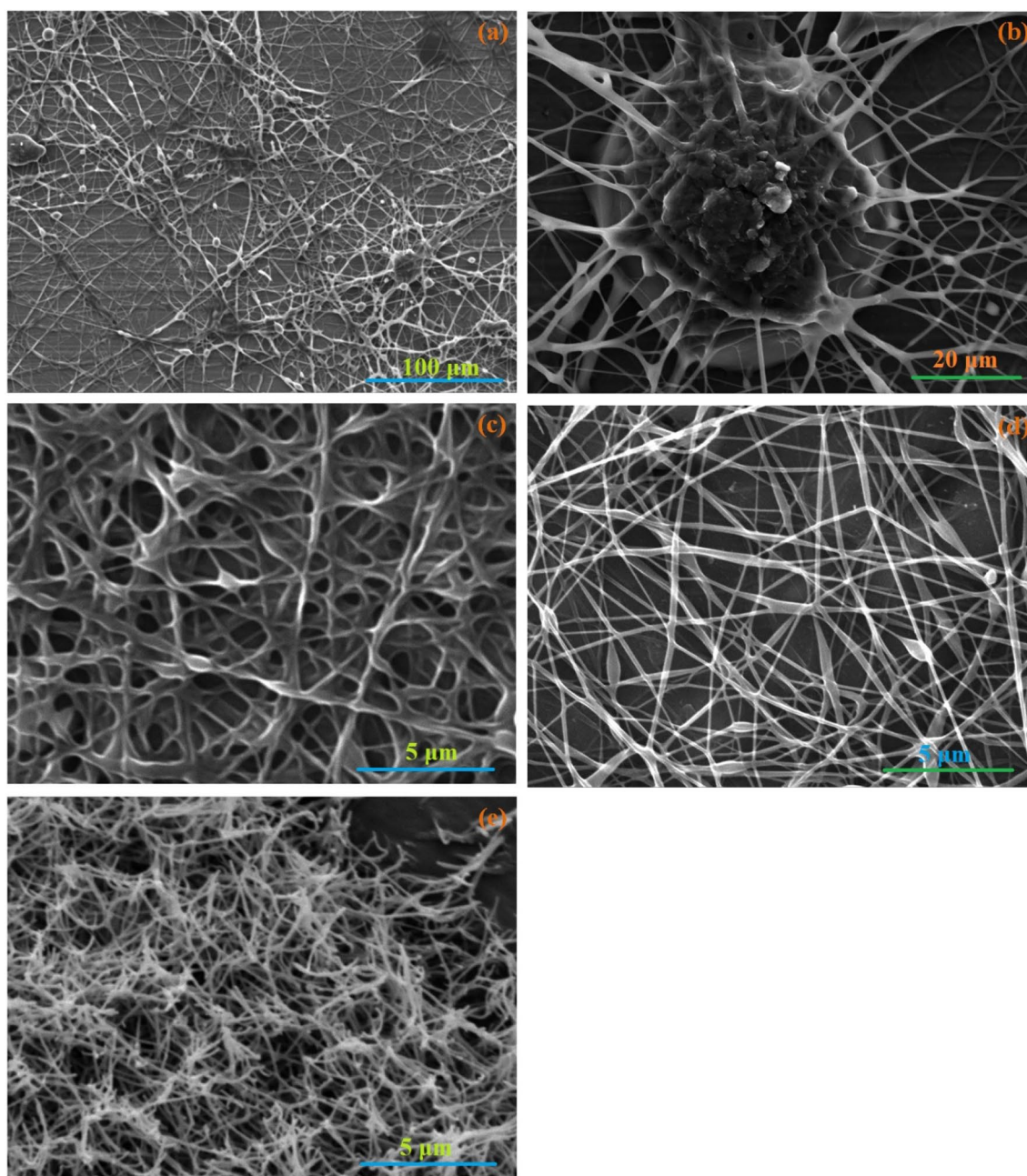


**Fig. 3** SEM image of PVA nanofibers prepared keeping the collector to syringe tip distance as 5 cm (a, b), 10 cm (c), 15 cm (d) and 20 cm (e)

### Effect of applied voltage on PVA nanofiber formation

The applied electrospinning voltage also should be within an optimum level, and at any other value, the formation would be disturbed, producing unevenly distributed fibers with different shapes. A critical applied voltage is required to initiate ejection of polymeric jet by overcoming the surface tension at the Taylor cone. The shape and stability of Taylor cone formation is varied affecting quality of scaffolds produced

(Li et al. 2008). The applied voltage was varied to 10, 12, 14 and 16 kV in the formation of PVA/honey hybrid scaffolds keeping a constant optimal distance 15 cm between tip and collector distance. At the applied voltages of 10 and 12 kV, solution was formed as bubbles and held stable at tip of capillary because of surface tension. These applied voltages were not beyond surface tension of the solution. Therefore, Taylor cone was not formed causing no formation of fiber. For an applied voltage of 14KV, though it is beyond critical voltage and surface tension of the solution,

the formed Taylor cone was not stable resulting in irregular deposits (Fig. 4a). However, applied voltage of 16 kV produced a stable Taylor cone ejecting smooth jet of solution producing defect-free uniform nanofibers on the collector plate (Fig. 4b). Hence, this particular optimal voltage was used for the further formation of PVA nano-fiber.

### Effect of solution concentration on the morphology of PVA/honey nanofiber

Solution concentration regulates fiber size and extrusion efficiency of the fiber from spinneret. Molecular weight, molecular density, and steric repulsion of molecules jointly determine the concentration property of the solution. It is also associated with other parameters such as needle size, applied voltage, and flow rate that determine the property of formed fiber. Concentration of honey in PVA solution was varied as 1, 2, 3 and 4 ml to form PVA/honey nanofibers at 16 kV with a flow rate of 0.001 ml/min. As shown in Fig. 5, the size of fibers formed has increased with the increase of honey concentration in PVA solution. This increase in fiber diameter exhibits the increased presence of honey in nanofibrous scaffolds. At higher concentration of honey (4 ml) with applied voltage (16 kV), a thicker and smooth nanofibrous scaffold was produced, indicating that there is no degenerative effect on honey due to higher voltage. Hence, a concentration of 4% (4 ml) honey was considered for further fabrication and application of PVA/honey nanofibrous scaffolds.

### UV–Vis spectrum of PVA and PVA/honey

UV–visible spectrum of PVA (Fig. 6) shows no absorption in the range of 400–1000 nm. This spectrum correlates with the work of Shipra Pandey team (Pandey et al. 2011), whereas UV spectrum of pure honey shows absorbance at 306 nm, which is slightly different from previous reports. This might

be due to the variation of origin of honey. The spectrum of PVA/honey reveals the absorption at 300 nm depending on the concentration in the fabricated PVA/honey scaffolds. The variation of absorption with honey concentration indicates the inclusion of honey in the PVA/honey hybrid scaffolds fabricated using the optimized condition. The UV–visible spectrum expressed the presence of honey in polymer scaffold that indicates the honey was not degenerated by highest applied voltage of 16KV given during electrospinning.

### FTIR spectroscopic analysis

Physicochemical properties of prepared samples were analyzed using Fourier transform infrared spectroscopy (FTIR) in 4000–400  $\text{cm}^{-1}$  wavenumber range as shown in Fig. 7. The PVA sample shows absorption bands at 2861 ( $-\text{CH}_2$ ), 1660 ( $-\text{OH}$ ), 1456 ( $\text{CH}_2$ ), 1309 ( $-\text{C}-\text{O}-\text{H}$ ), 3233 (alcohol OH stretch), which is in good agreement with the literature (Abd El-aziz et al. 2017; Awada and Daneault 2015)]. Honey incorporated PVA scaffolds also showed absorbance peaks similar to PVA bands, but with increased intensity. The absorption bands of PVA/honey hybrid scaffolds observed at 3320/ $\text{cm}$  and 2900/ $\text{cm}$  indicate the O–H stretching of water and C–H bonds of sugar molecules respectively, whereas the band obtained at 3169  $\text{cm}^{-1}$  infers amide N–H bond of honey. The C–O bond of protein molecules in honey was observed at 1857  $\text{cm}^{-1}$ , C–N stretching and deformation of C–C–H of PVA molecules showed bands, respectively, at 1313/ $\text{cm}$  and 1240/ $\text{cm}$ . The band of PVA at 1097/ $\text{cm}$  was shifted to 1082/ $\text{cm}$  due to the stretching of C–O bond of honey. Similarly, the bands located at 710 (C–H), 705 (C–H), 741 (C–H) are the C–H bending of sugar molecules indicating the presence of honey in the fibre. Honey incorporated scaffolds showed increased absorption peaks directly depending on honey concentration. The increase of absorption peaks for honey-incorporated scaffolds indicates

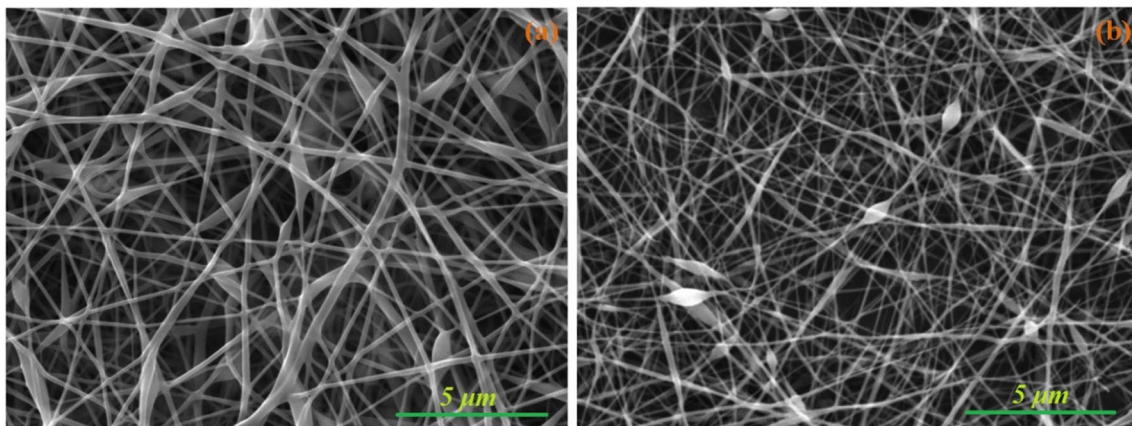


**Fig. 4** SEM image of PVA scaffold formed at different applied voltages

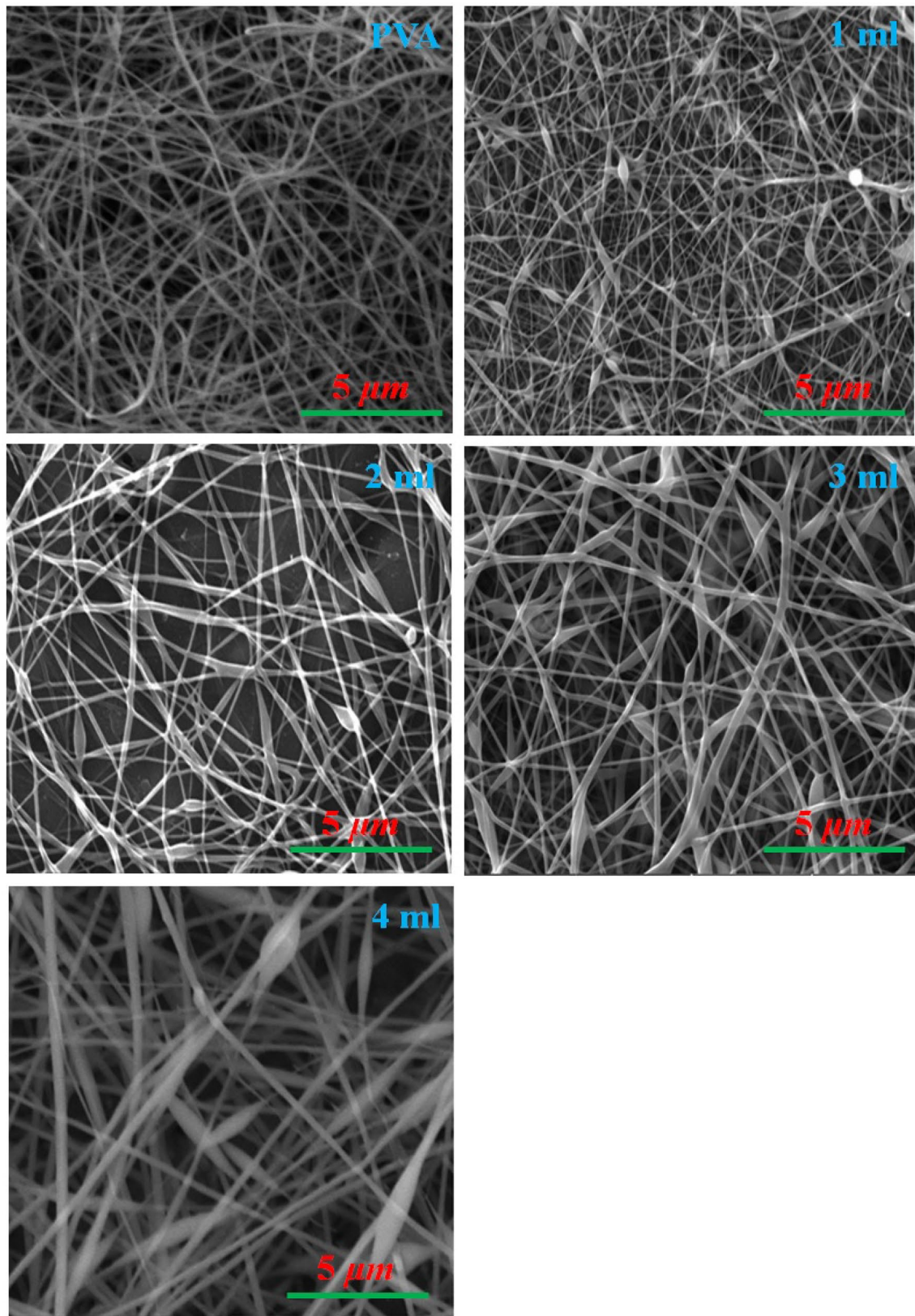


**Fig. 5** SEM images of PVA/honey hybrid nanofibrous scaffolds of different honey concentrations



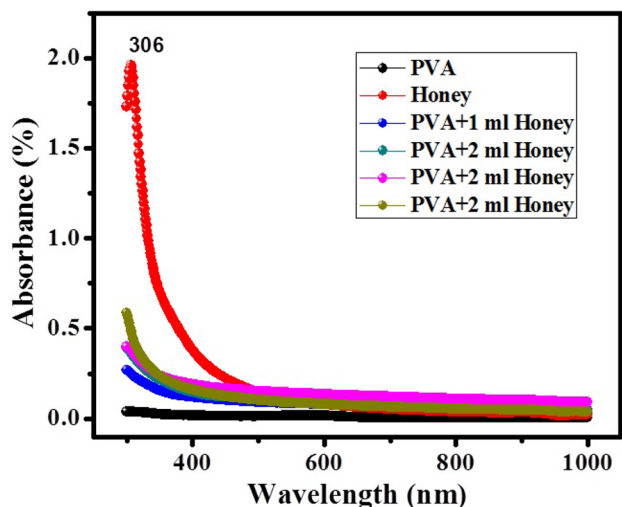


**Fig. 6** UV–visible absorption spectrum of PVA, honey and PVA/honey scaffold with different honey concentrations

the increased amount of hydrogen-bonded hydroxyl groups due to the presence of sugar molecules in it. Hence, honey-incorporated PVA scaffolds show increased absorption of hydroxyl group in response to the different concentration of honey. These changes in absorption spectra show the better affinity between PVA and honey in PVA/honey membrane. A similar increase of absorbance due to inclusion of honey with PVA was also reported by Santos et al. (Neres Santos et al. 2019). Different absorbance bands of PVA, pure honey and PVA/honey hybrid are shown in Table 2.

**X-ray diffraction analysis**

Crystalline and structural properties of prepared PVA and PVA/honey nano-fibrous scaffolds were determined using XRD diffraction spectrum of nanofibers and it is shown with smoothed curve in Fig. 8. The sharp spike-like peaks observed at  $2\theta = 11.2^\circ, 12.5^\circ, 19.4^\circ, 20.7^\circ, 23.4^\circ, 25.2^\circ$  and  $28.6^\circ$  are correspond to PVA, and other two high-intensity peaks were at  $37.92^\circ$  and  $44.26^\circ$  are from aluminum foil used as support (Elkomy et al. 2016; Park et al. 2012; Tang et al. 2015). The honey-included sample additionally shows

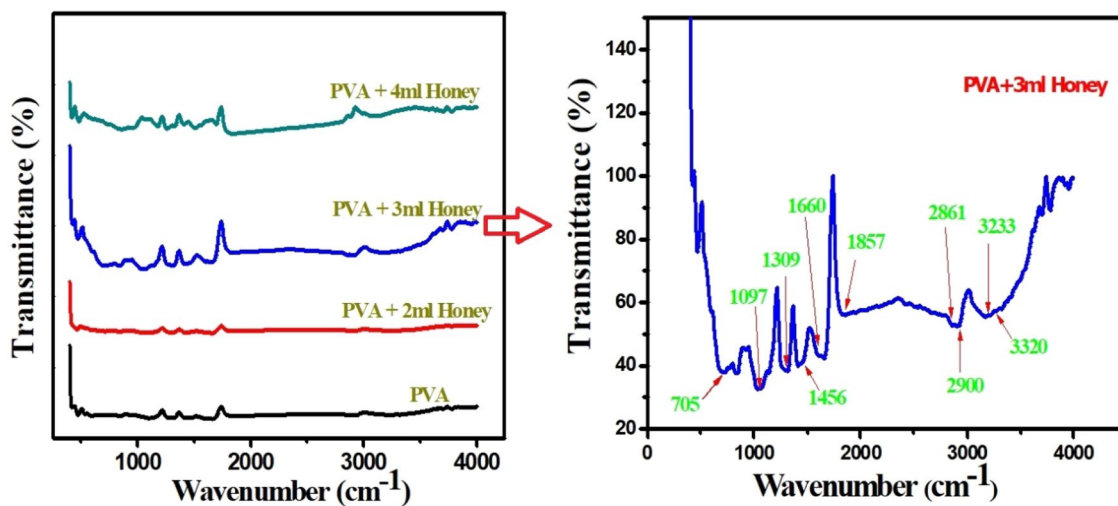


**Fig. 7** a FTIR spectrum of PVA and PVA/honey scaffolds for different honey concentration, b magnified view of 3 ml honey-employed scaffold

**Table 2** PVA and PVA/honey nanofiber FTIR absorption wavenumbers

Functional groups	PVA	Pure honey	PVA + 1 ml honey	PVA + 2 ml honey	PVA + 3 ml honey	PVA + 4 ml honey
-O–H	3233	3272	3305	3230	3320	3414
-C–H	2861	2932	2939	2923	2900	2980
-O–H	1660	1643	1689	1656	1657	1693
-CH <sub>2</sub>	1461	1416	1419	1414	1414	1407
-O–H	1309	1344	–	1312	1313	1325
-C–O	1097	–	–	–	–	–
-C–H (sugar)	–	775	–	710	705	741

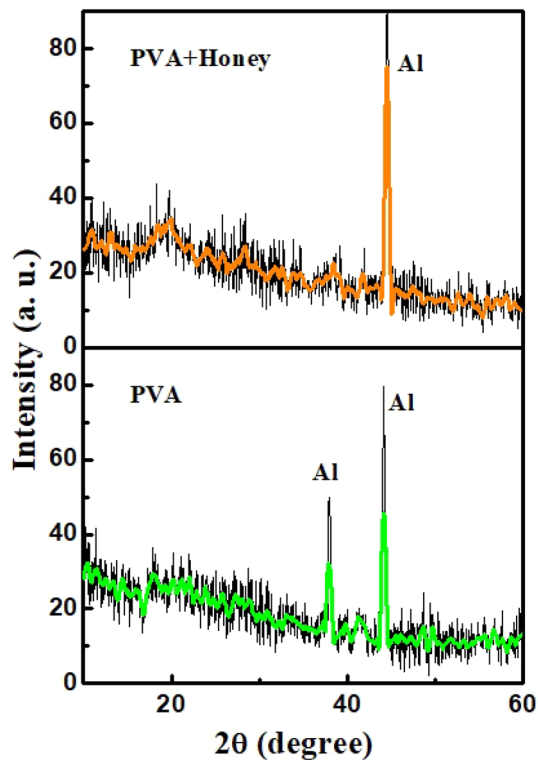


**Fig. 8** XRD spectrum of PVA, honey, PVA + 1 ml honey, PVA + 2 ml honey, PVA + 3 ml honey and PVA + 4 ml honey

a wide peak at around  $20^\circ$  indicating the inclusion honey. Moreover, this wide peak was increased and slightly shifted to lower angle for the increase of honey concentration. This justifies the inclusion of honey and its increased content in the fabricated scaffolds.

### Conductivity of PVA/honey hybrid fiber and pH variation of honey

To check the effect honey with PVA, the conductivity of honey extracted from honey/PVA hybrid fiber of different honey concentration was measured. Figure 9 indicates the conductivity change of honey solution with respect to concentration of honey. As seen in the figure, conductivity of the PVA/honey solution was increased with the increase in honey concentration, indicating that the increased releasing profile of honey at higher concentration. That is, the higher concentration honey-incorporated PVA nanofibrous scaffolds might have higher releasing kinetics. The pH value of honey is also playing a role in wound healing process. Usually, the pH value of honey is in between 3.4 and 6.1 depending on the condition formed, but the honey that was used showed a pH of 5.9, this high-pH honey was highly suitable for the inhibition of bacterial growth. Moreover,

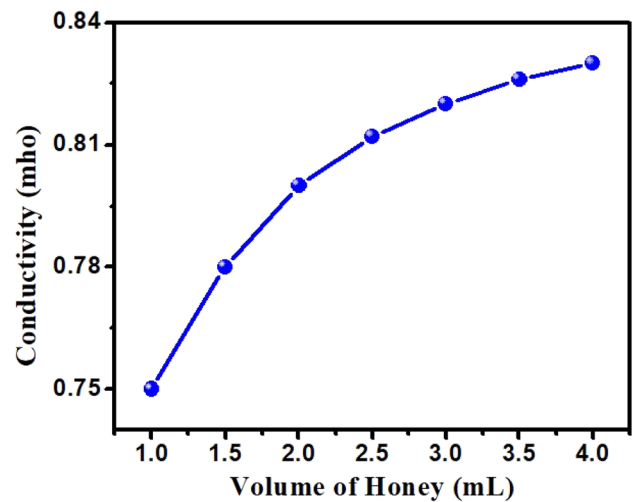


**Fig. 9** Variation honey conductivity with concentration

this acidic pH of honey can also play a significant role in the chronic wound healing mechanism.

### In vitro releasing kinetics analysis

Honey release from the electro-spun PVA nanofibers of two different thickness samples as a function of immersion duration is shown in Fig. 10. As seen, the releasing behaviors of the samples are similar for the first two intervals of duration. Honey release from 2-h-spun nanofibers was gradually increased up to 4th day and then the release was saturated from the 5th day onwards. Releasing profile of 4-ml 4-h-spun fiber was high compared to releasing kinetics of 2-h-electrospun nanofibers. The burst release of honey from the fibers with 5 days of immersion was due to high

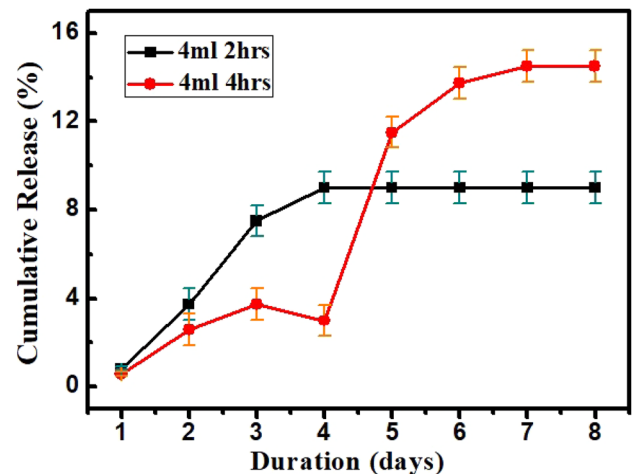


**Fig. 10** Releasing kinetics of PVA + 4 ml honey nanofibers of two different thickness with different spinning duration of 2 h and 4 h

diffusion of honey in the scaffolds. The releasing behavior of nanofibrous scaffolds were based on the swelling property of the fiber as reported by Maleik et al. (Maleki et al. 2013). In this experiment, it was inferred that the molecules of honey were released from the fibers immediately after the swelling of PVA nanofibers. The honey concentration in the immersion medium was increased with the increase in thickness of the nanofibrous scaffolds. The diffusion of honey and its increased osmolality was the main factor for its releasing behavior. Therefore, high concentration of honey-incorporated thicker PVA nanofiber scaffolds might have higher releasing kinetics as inferred in the conductivity study.

### Swelling property analysis

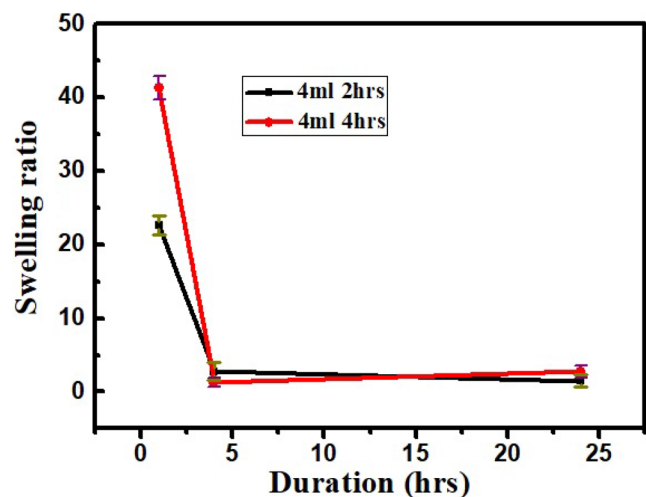
When concentration of honey in scaffold was increased, its releasing rate from scaffold was also increased. This honey release attributes weight loss in the scaffolds due to the breakdown of polymeric network and release of active components. Osmolality property of honey enhances water uptake capability of scaffolds as a result of hydrolysis of PVA causing swelling of scaffolds (Tavakoli and Tang 2017). PVA polymeric network breakdown results in mechanical properties loss causing weight loss of the synthesized scaffolds. Therefore, the weight loss occurred in PVA/honey nanofibers because of hydrolysis and leaching of PVA. It appeared that the release of a drug was mainly controlled by the swelling behavior of the fibers (Maleki et al. 2013). When fibers start to swell, the drug molecules were dissolved and released from the fiber. Therefore, the measurement of swelling ratio gives the capability of wound dressing in infection control and wound healing; it depends on biological properties of wound and wound dressing robustness against its environment. Swelling

behavior analysis of PVA/honey of two different thickened samples is shown in Fig. 11. As it shows reduction of swelling ratio, the prepared scaffold is stable for longer time.

### MTT cytotoxicity assay

Cell growth and its proliferation on the nanofibrous scaffolds were determined using MTT assay. The percentage of cell viability and its growth rate had been evaluated using MTT assay on L929 cells for 3 days of incubation. The dissolved MTT produced the formazan crystals in the culture well through the enzyme formation in the mitochondria of the viable cells. L929 mouse fibroblast cell line was cultured at different concentrations of honey-incorporated nanofiber (500–1.95  $\mu\text{g}$ ) extract solution and the toxicity of cells on the nanofibers was evaluated by measuring the percentage of viable cells present after 48 h of incubation. It was observed that honey-loaded nanofibers exposed cell viability in the range of 99–90% for lower to higher concentration, respectively. The four different concentrations of honey/PVA nanofibrous scaffolds showed highest cell viability of 85–90% for highest concentration in all the experiments and revealed that there were not any lethal cells found. The MTT results comprehended that honey-loaded electrospun nanofibrous scaffold is proposed to be the appropriate substrate for the cellular adhesion, growth, and proliferation primarily by its biomimicking property of ECM. Hence, we suggest that the highest cell viability of PVA/honey nanoscaffolds was mainly due to the presence of the honey which is an organic compound and it could be a worthy and more suitable Band-Aid for the treatment of chronic wounds. The MTT assay mechanism graph is shown in Fig. 12

**Fig. 11** Swelling behavior of PVA/honey nanofiber for different time intervals



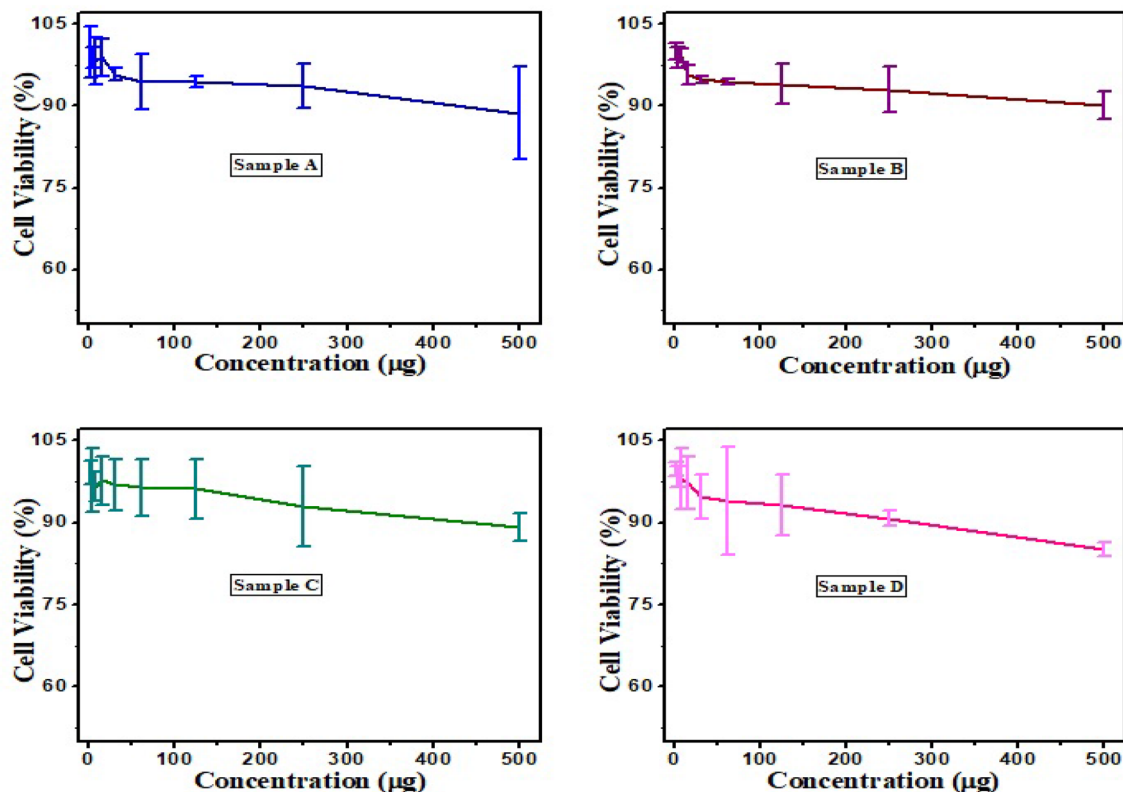


**Fig. 12** Cell viability percentage with higher concentration of 250 and 500 µg (a) 1 ml honey / PVA nanofiber, (b) 2 ml honey/PVA, (c) 3 ml honey/PVA, (d) 4 ml honey/PVA

## Conclusion

Polyvinyl alcohol nanoscaffolds were synthesized using electrospinning after optimizing the process and solution parameters to incorporate honey in it. Based on the experimental results, the distance between collector and syringe tip, applied voltage and solution flow rate selected for the preparation of honey/PVA scaffolds were 15 cm, 16 kV and 0.001 mL/min, respectively. High concentration of honey (4%) produced good results with increased releasing profile in in vitro analysis. Swelling analysis inferred high concentration of honey is desirable for weight loss of scaffolds due to the release of active components and hydrolysis of PVA. The inclusion of honey with PVA scaffold can show inhibition activity for proteases in chronic wounds and prevent the bacterial infection that occurred over the wound site, and inhibit biofilm formation. This work suggests that the honey-incorporated nanofibrous scaffold activates the prevention of biofilm formation and fast healing of chronic wounds due to efficient osmolality effect.

## Compliance with ethical standards

**Conflict of interest** There are no conflicts to declare.

## References

- AbdElaziz AM, ElMaghraby A, Taha NA (2017) Comparison between polyvinyl alcohol (PVA) nanofiber and polyvinyl alcohol (PVA) nanofiber/hydroxyapatite (HA) for removal of Zn<sup>2+</sup> ions from wastewater. *Arab J Chem* 10:1052–1060. <https://doi.org/10.1016/j.arabjc.2016.09.025>
- Albaridi NA (2019) Antibacterial potency of honey. *Int J Microbiol* 2019:10. <https://doi.org/10.1155/2019/2464507>
- Anand S, Deighton M, Livanos G, Morrison PD, Pang ECK, Mantri N (2019) Antimicrobial activity of Agastache honey and characterization of its bioactive compounds in comparison with important commercial honeys. *Front Microbiol.* <https://doi.org/10.3389/fmicb.2019.00263>
- Anderson DEJ, Truong KP, Hagen MW, Yim EKF, Hinds MT (2019) Biomimetic modification of poly(vinyl alcohol): encouraging endothelialization and preventing thrombosis with antiplatelet monotherapy. *Acta Biomater* 86:291–299. <https://doi.org/10.1016/j.actbio.2019.01.008>

- Awada H, Daneault C (2015) Chemical modification of poly(vinyl alcohol) in water applied. *Sciences* 5:840–850
- Biswas A, Amarajeewa M, Senapati S, Sahu M, Maiti P (2018) Sustained release of herbal drugs using biodegradable scaffold for faster wound healing and better patient compliance. *Nanomedicine* 14:2131–2141. <https://doi.org/10.1016/j.nano.2018.07.003>
- Chao CY, Mani MP, Jaganathan SK (2018) Engineering electrospun multicomponent polyurethane scaffolding platform comprising grape seed oil and honey/propolis for bone tissue regeneration. *PLoS ONE* 13:e0205699. <https://doi.org/10.1371/journal.pone.0205699>
- Costa MF, Durco AO, Rabelo TK, Barreto RSS, Guimaraes AG (2019) Effects of carvacrol, thymol and essential oils containing such monoterpenes on wound healing: a systematic review. *J Pharm Pharmacol* 71:141–155. <https://doi.org/10.1111/jphp.13054>
- Elkomy GM, Mousa SM, Mostafa HA (2016) Structural and optical properties of pure PVA/PPY and cobalt chloride doped PVA/PPY films. *Arab J Chem* 9:S1786–S1792. <https://doi.org/10.1016/j.arabjc.2012.04.037>
- ElZaher NA, Osiris WG (2005) Thermal and structural properties of poly(vinyl alcohol) doped with hydroxypropyl cellulose. *J Appl Polym Sci* 96:1914–1923. <https://doi.org/10.1002/app.21628>
- Gupta D, Jassal M, Agrawal AK (2016) The electrospinning behavior of poly(vinyl alcohol) in DMSO–water binary solvent mixtures. *RSC Adv* 6:102947–102955. <https://doi.org/10.1039/C6RA15017A>
- Hassiba AJ et al (2017) Synthesis, characterization, and antimicrobial properties of novel double layer nanocomposite electrospun fibers for wound dressing applications. *Int J Nanomed* 12:2205–2213. <https://doi.org/10.2147/ijn.S123417>
- Kwakman PHS, Velde AAT, Boer LD, Speijer D, Vandenbroucke-Grauls CMJE, Zaat SAJ (2010) How honey kills bacteria. *FASEB J* 24:2576–2582. <https://doi.org/10.1096/fj.09-150789>
- Li N, Qin X-H, Lin L, Wang S-Y (2008) The effects of spinning conditions on the morphology of electrospun jet and nonwoven membrane. *Polym Eng Sci* 48:2362–2366. <https://doi.org/10.1002/pen.21188>
- Li J et al (2017) Polymer materials for prevention of postoperative adhesion. *Acta Biomater* 61:21–40. <https://doi.org/10.1016/j.actbio.2017.08.002>
- Lin SY, Chen KS, Run-Chu L (2001) Design and evaluation of drug-loaded wound dressing having thermoresponsive, adhesive, absorptive and easy peeling properties. *Biomaterials* 22:2999–3004. [https://doi.org/10.1016/S0142-9612\(01\)00046-1](https://doi.org/10.1016/S0142-9612(01)00046-1)
- Long Y, Wei H, Li J, Yao G, Yu B, Ni D, Gibson AL, Lan X, Jiang Y, Cai W, Wang X (2018) Effective wound healing enabled by discrete alternative electric fields from wearable nanogenerators. *ACS Nano* 12(12):12533–12540
- Maleki H, Gharehaghaji AA, Dijkstra PJ (2013) A novel honey-based nanofibrous scaffold for wound dressing application. *J Appl Polym Sci* 127:4086–4092. <https://doi.org/10.1002/app.37601>
- Mama M, Teshome T, Detamo J (2019) Antibacterial activity of honey against methicillin-resistant staphylococcus aureus: a laboratory-based experimental study. *Int J Microbiol* 2019:9. <https://doi.org/10.1155/2019/7686130>
- Meo SA, AlAsiri SA, Mahesar AL, Ansari MJ (2017) Role of honey in modern medicine. *Saudi J Biol Sci* 24:975–978. <https://doi.org/10.1016/j.sjbs.2016.12.010>
- MindenBirkenmaier BA, Bowlin GL (2018) Honey-based templates in wound healing and tissue engineering. *Bioengineering* 5:46
- Moore OA, Smith LA, Campbell F, Seers K, McQuay HJ, Moore RA (2001) Systematic review of the use of honey as a wound dressing. *BMC Complement Altern Med* 1:2. <https://doi.org/10.1186/1472-6882-1-2>
- Moura LIF, Dias AMA, Carvalho E, de Sousa HC (2013) Recent advances on the development of wound dressings for diabetic foot ulcer treatment a review. *Acta Biomater* 9:7093–7114. <https://doi.org/10.1016/j.actbio.2013.03.033>
- Movassaghi S, Sharifi ZN, Koosha M, Abdollahifar MA, Fathollahipour S, Tavakoli J, Abdi S (2019) Effect of Honey/PVA Hydrogel Loaded by Erythromycin on Full-Thickness. *Galen Med J* 2019:8. <https://doi.org/10.31661/gmj.v8i0.1362>
- NeresSantos AM et al (2019) Physically cross-linked gels of PVA with natural polymers as matrices for manuka honey release in wound-care applications. *Materials (Basel)* 12:10. <https://doi.org/10.3390/ma12040559>
- Nethi SK, Das S, Patra CR, Mukherjee S (2019) Recent advances in inorganic nanomaterials for wound-healing applications *Biomaterials*. *Science* 7:2652–2674. <https://doi.org/10.1039/C9BM00423H>
- Oktay B, Kayaman-Apohan N, Erdem-Kuruca S (2014) Fabrication of nanofiber mats from electrospinning of functionalized polymers. *IOP Conf Ser* 64:012011. <https://doi.org/10.1088/1757-899x/64/1/012011>
- Pandey S, Pandey SK, Parashar V, Mehrotra GK, Pandey AC (2011) Ag/PVA nanocomposites: optical and thermal dimensions. *J Mater Chem* 21:17154–17159. <https://doi.org/10.1039/C1JM13276H>
- Park JH et al (2012) Poly(vinyl alcohol)/montmorillonite/silver hybrid nanoparticles prepared from aqueous solutions by the electro-spraying method. *J Compos Mater* 47:3367–3378. <https://doi.org/10.1177/0021998312465100>
- Pinto SC et al (2015) Stryphnodendron adstringens: clarifying wound healing in streptozotocin-induced diabetic rats. *Planta Med* 81:1090–1096. <https://doi.org/10.1055/s-0035-1546209>
- Putu EPK, Ida BADP, Ratna RNR (2018) Honey clinically stimulates granulation and epithelialization in chronic wounds: a report of two cases. *Med J Indones* 27:5. <https://doi.org/10.13181/mji.v27i1.1457>
- Qi J, Zhang H, Wang Y, Mani MP, Jaganathan SK (2018) Development and blood compatibility assessment of electrospun polyvinyl alcohol blended with metallocene polyethylene and *Plectranthus amboinicus* (PVA/mPE/PA) for bone tissue engineering. *Int J Nanomed* 13:2777–2788. <https://doi.org/10.2147/ijn.S151242>
- Rezvani Z, Venugopal JR, Urbanska AM, Mills DK, Ramakrishna S, Mozafari M (2016) A bird's eye view on the use of electrospun nanofibrous scaffolds for bone tissue engineering: current state-of-the-art, emerging directions and future trends. *Nanomedicine* 12:2181–2200. <https://doi.org/10.1016/j.nano.2016.05.014>
- Samarghandian S, Farkhondeh T, Samini F (2017) Honey and health: a review of recent clinical research. *Pharmacogn Res* 9:121–127. <https://doi.org/10.4103/0974-8490.204647>
- Sarhan WA, Azzazy HME, ElSherbiny IM (2016) The effect of increasing honey concentration on the properties of the honey/polyvinyl alcohol/chitosan nanofibers. *Mater Sci Eng* 67:276–284. <https://doi.org/10.1016/j.msec.2016.05.006>
- Son YJ, Tse JW, Zhou Y, Mao W, Yim EKF, Yoo HS (2019) Biomaterials and controlled release strategy for epithelial wound healing. *Biomaterials Science* 7:4444–4471. <https://doi.org/10.1039/C9BM00456D>
- Song JJ, Salcido R (2011) Use of honey in wound care: an update. *Adv Skin Wound Care* 24:40–44. <https://doi.org/10.1097/01.Asw.0000392731.34723.06>
- Stejskalová A, Almquist BD (2017) Using biomaterials to rewire the process of wound repair biomaterials. *Science* 5:1421–1434. <https://doi.org/10.1039/C7BM00295E>
- Suwantong O, Pankongadisak P, Deachathai S, Supaphol P (2012) Electrospun poly(l-lactic acid) fiber mats containing a crude *Garcinia cowa* extract for wound dressing applications. *J Polym Res* 19:9896. <https://doi.org/10.1007/s10965-012-98963>

- Tang C-M, Tian Y-H, Hsu S-H (2015) Poly(vinyl alcohol) nanocomposites reinforced with bamboo charcoal nanoparticles: mineralization behavior and characterization. *Materials* 8:4895–4911
- Tavakoli J, Tang Y (2017) Honey/PVA hybrid wound dressings with controlled release of antibiotics: structural, physico-mechanical and in-vitro biomedical studies. *Mater Sci Eng C Mater Biol Appl* 77:318–325. <https://doi.org/10.1016/j.msec.2017.03.272>
- Wang S, Hu F, Li J, Zhang S, Shen M, Huang M, Shi X (2018) Design of electrospun nanofibrous mats for osteogenic differentiation of mesenchymal stem cells. *Nanomedicine* 14:2505–2520. <https://doi.org/10.1016/j.nano.2016.12.024>
- Xiao M, Chery J, Frey MW (2018) Functionalization of electrospun poly(vinyl alcohol) (PVA) nanofiber membranes for selective chemical capture. *ACS Appl Nano Mater* 1:722–729. <https://doi.org/10.1021/acsnm.7b00180>
- Yao G et al (2019) Self-activated electrical stimulation for effective hair regeneration via a wearable omnidirectional pulse generator. *ACS Nano* 13:12345–12356. <https://doi.org/10.1021/acsnano.9b03912>
- Zanier E, Bordoni B (2015) A multidisciplinary approach to scars: a narrative review. *J Multidiscip Healthc* 8:359–363. <https://doi.org/10.2147/jmdh.S87845>
- Zargham S, Bazgir S, Tavakoli A, Rashidi AS, Damerchely R (2012) The effect of flow rate on morphology and deposition area of electrospun nylon 6 nanofiber. *J Eng Fibers Fabr* 7:54. <https://doi.org/10.1021/acsnano.8b07038>

**Publisher's Note** Springer Nature remains neutral with regard to jurisdictional claims in published maps and institutional affiliations.